Chemical Physics 473 (2016) 1–10

Contents lists available at ScienceDirect

Chemical Physics

journal homepage: www.elsevier.com/locate/chemphys

Two-exciton excited states of *J*-aggregates in the presence of exciton–exciton annihilation

B. Levinsky [a], B.D. Fainberg [a,b,*], L.A. Nesterov [c,d], N.N. Rosanov [c,d,e]

[a] Physics Department, Holon Institute of Technology, 52 Golomb St., Holon 5810201, Israel
[b] School of Chemistry, Tel-Aviv University, Tel-Aviv 69978, Israel
[c] ITMO University, St. Petersburg 197101, Russia
[d] Vavilov State Optical Institute, St. Petersburg 199034, Russia
[e] Ioffe Physical-Technical Institute, Russian Academy of Sciences, St. Petersburg 194021, Russia

ARTICLE INFO

Article history:
Received 10 December 2015
In final form 7 April 2016
Available online 19 April 2016

Keywords:
Excitons
Two-exciton states
Exciton–exciton annihilation
Coherent decay

ABSTRACT

We study decay of two-exciton states of a *J*-aggregate that is collective in nature. We use mathematical formalism based on effective non-Hermitian Hamiltonian suggested in nuclear theory. We show that decay of two-exciton states is strongly affected by the interference processes in the exciton–exciton annihilation. Our evaluations of the imaginary part of the effective Hamiltonian show that it exceeds the spacing between real energies of the two-exciton states that gives rise to the transition to the regime of overlapping resonances supplying the system by the new collectivity – the possibility of coherent decay in the annihilation channel. The decay of two-exciton states varies from twice bimolecular decay rate to the much smaller values that is associated with population trapping. We have also considered the corresponding experiment in the framework of our approach, the picture of which appears to be more complex and richer than it was reasoned before.

1. Introduction

Collective mechanism of excitation of linear molecular *J*-aggregates determines their unique nonlinear optical properties [1]. Among them the *N*-fold enhancement of the spontaneous emission rate and the N^2 scaling of the cubic hyperpolarizability, where *N* is the number of molecules in the aggregate. The reason is the collective (excitonic) character of aggregate eigenfunctions. The collective mechanism also results in a bistable behavior of molecular *J*-aggregates [2,3], and dissipative solitons [4,5] that arise in these structures under resonant laser excitation. These solitons are nanosized structures, which are localized almost within the region of a single molecule, which opens up possibilities for creating subminiature memory cells.

The bistability and dissipative solitons predicted are strongly affected by the process of excitonic annihilation, which plays a role with increasing pump intensity [6–9]. Exciton annihilation in molecular crystals was studied in Refs. [6,7], and in dye *J*-aggregates in Refs. [10–12] experimentally and [13,14] theoretically. In Ref. [15] the anharmonic oscillator approach was developed to model exciton annihilation in pigment-protein complexes. Consider two-exciton excitation of a molecular aggregate. The scheme of the exciton–exciton annihilation process through a third molecular level [13,14] includes two steps. In the first step, one excited molecule goes to the ground state $|g\rangle$ while another excited molecule passes to the third level $|f\rangle$ (due to the energy conservation). The second step is the radiationless relaxation of the third level $|f\rangle$ to the ground $|g\rangle$ and excited $|e\rangle$ states of the transition of interest. It is assumed that the third level $|f\rangle$ is vibronic in its nature and decays very rapidly transferring its energy to the excited $|e\rangle$ and ground $|g\rangle$ levels with the rates Γ_{fe} and Γ_{fg}, respectively.

In Ref. [3] an ensemble of molecular aggregates in a thin film was considered using an effective four-level scheme, and in Refs. [2,4,5] *J*-aggregates were described using a local field approximation [16], in which a chain of molecules is described by a system of Bloch equations for one-particle density matrices. In this case, the interaction between molecules is derived using the classical expression for the retarding interaction between a system of dipoles by which molecules are modeled. In addition, the above mentioned interaction that leads to exciton–exciton annihilation is also introduced into the system (usually phenomenologically). As a rule, in the system of equations obtained in this way, only two particle interactions are taken into account, which are

* Corresponding author at: Physics Department, Holon Institute of Technology, 52 Golomb St., Holon 5810201, Israel.

http://dx.doi.org/10.1016/j.chemphys.2016.04.006
0301-0104/

presented in the factorized form, i.e., without taking into account correlations between molecules.

However, the system of equations for J-aggregates can also be derived from first principles. In this case, a hierarchy of mutually coupled equations for the expectation values of products of operators that refer to different molecules of the chain arises [16]. This system contains expectation values beginning from one particle and ending with N particle expectation values (N is the number of molecules in the chain, and $N \gg 1$). An important aspect of this problem is that the third level of molecules is a system of a large number of vibrational sublevels, interaction with which leads to dissipation of energy and to irreversibility of the exciton–exciton annihilation process. If this interaction is correctly taken into account from the first principles, the equations of motion will acquire a number of multiparticle contributions that describe the relaxation of the system related to the exciton–exciton annihilation [17] but that, however, are absent in the purely phenomenological picture. In Ref. [17] we took the two-particle expectation values into account directly in the hierarchical system of equations. In general, taking the interaction with a third level of molecules into account leads to the appearance not only of three-particle but also of four-particle relaxation terms in equations of motion. As a consequence, the exciton–exciton annihilation processes also result in mixing the optical transitions in J -aggregates.

Furthermore, equations of Ref. [17] were written in the site representation. However, the applicability of the bimolecular theory, which implies the approach of two excitons before they annihilate, is questionable [13,14]. Authors of earlier pioneering work [13] obtained an insight into the possible channels of excitonic annihilation at low temperatures, when one-dimensional excitons become localized in the part of the aggregate due to a weak static disorder. They proposed an alternative channel of excitonic annihilation that was inversely proportional to the cube of the localization length. In the present work following Ref. [13] we also take the localization of one-dimensional excitons in the part of the aggregate into consideration. However, in contrast to Ref. [13], we consider rather eigenstates of the effective non–Hermitian Hamiltonian [18] including the decay due to the exciton–exciton annihilation, than eigenstates obtained by diagonalization of the Hamiltonian of a J-aggregate with respect to the dipole–dipole interaction between its molecules, Eq. (6) below. This is an important generalization of the theory when the value of the dipole–dipole interaction between molecules of a J-aggregate (see Eq. (6) below) $|J|$ is not much larger than the probability of bimolecular decay w_a (see below). By this means the spectrum of the problem under consideration should be found with taking the decay due to the exciton–exciton annihilation into account. In addition, the exciton–exciton annihilation is described by non-diagonal relaxation matrix due to both the relaxation of two-particle variables associated with that of three- and four-particles variables, and using basis $|\mu\nu\rangle$ in which even the relaxation of two-particle variables becomes non-diagonal. The appropriate mathematical formalism for the description of this physics is provided by the effective non–Hermitian Hamiltonian [18] suggested in nuclear theory that will be used in the present work. This formalism is highly efficient for the study of collective states demonstrating various behaviors, the two extreme cases of which are super-radiance by Dicke [19,20] and the population trapping [21,18]. At the end of the 20th century it was understood that the physics underlying super-radiance is much more general and can find broad applications in various regions of the quantum world [18].

For our goal, the main lesson is that the quantum states can be coupled also through the continuum of open decay channels. Since the continuum coupling determines the width 2α, or the lifetime $\tau \sim \hbar/(2\alpha)$, the states become quasi-stationary and can be characterized by a complex energy, $\widetilde{E} = E - i\alpha$. Similar to standard perturbation theory, the efficiency of coupling is determined by the ratio of the coupling strength to the energy spacing between the coupled states. If the width 2α is of the order of, or exceeds, the spacing between real energies E, coupling through the continuum turns out to be effectively strong. This transition to the regime of overlapping resonances supplies the system by the new collectivity - the possibility of coherent decay [18].

The paper is organized as follows. We start with the model in Section 2. In Section 3 we consider the evolution of the two-exciton excited states and specify the effective non–Hermitian Hamiltonian. Then we present the results of the numerical diagonalization of the effective Hamiltonian and discuss them, Section 4. In Section 5 we compare our results with previous calculations and experiment. In Section 6, we briefly conclude.

2. Model and Hamiltonian

Consider a linear chain that consists of N three-level molecules. Assume that the lowest state of each molecule is determined by the state vector $|g\rangle$, and the energy of this state is E_g. Correspondingly, the excited state will be determined by the state vector $|e\rangle$ with energy E_e. State vectors $|mg\rangle$ and $|me\rangle$ correspond to a molecule that is located at site m of the chain. Using these vectors, we can construct the following operators of creation and annihilation for each molecule: $B_m = |mg\rangle\langle me|$ is the operator that describes the annihilation of an excitation in molecule m at level e, and $B_m^\dagger = |me\rangle\langle mg|$ is the operator that describes the creation of an excitation in molecule m to level e. Furthermore, the upper level f of a molecule in the system of three-level molecules is a vibronic, and, to correctly perform calculations, we should take into account its structure. We will assume that upper level f consists of a series of sublevels ν, which correspond to different vibrational states and which are characterized by the density of states $\rho(E) = \sum_\nu \delta(E - E_{f\nu})$ necessary for the calculation of the transition probabilities. As a result, the third state will be determined by state vectors $|f\nu\rangle$ with energies $E_{f\nu}$ where $E_{f\nu} > E_e > E_g$. In a similar manner, we shall also define the following operators: $D_{m\nu} = |me\rangle\langle mf\nu|$, and $D_{m\nu}^\dagger = |mf\nu\rangle\langle me|$. In Ref. [17] the processes of exciton–exciton annihilation were described by the following Hamiltonian

$$H_{annih} = \sum_{\substack{k\neq l \\ \nu}} \left(V_{kl} B_k D_{l\nu}^+ + V_{lk} D_{l\nu} B_k^+\right) \tag{1}$$

The two-exciton state corresponding to the excitation of sites m and n can be written as $|mene\rangle = B_m^\dagger B_n^\dagger |mg\rangle|ng\rangle$. The energy of this state will be close to the energy $|kf\nu\rangle$ of any site k. Therefore, we shall seek the two-exciton wave function in the form

$$\Psi = \sum_{m>n} C_{mn} |mene\rangle \prod_{k\neq m,n} |kg\rangle + \sum_{m,\nu} d_{m\nu} |mf\nu\rangle \prod_{k\neq m} |kg\rangle \tag{2}$$

where C_{mn} and $d_{m\nu}$ are the amplitudes of the corresponding states. The evolution of two-exciton wave function Ψ

$$i\hbar \frac{d\Psi}{dt} = H\Psi \tag{3}$$

is determined by the Hamiltonian

$$H = H_0 + H_{int} + H_{annih} \tag{4}$$

Here

$$H_0 = \sum_m \hbar\omega_{me,g} B_m^+ B_m + \sum_{m,\nu} \hbar\omega_{mf\nu,g} D_{m\nu}^+ D_{m\nu} \tag{5}$$

is the Hamiltonian of free molecules of a J-aggregate,

$$H_{int} = \hbar\sum_{m\neq n}\left(J^{gege}_{mn}B^{\dagger}_{m}B_{n} + J^{*gege}_{mn}B^{\dagger}_{n}B_{m}\right) \quad (6)$$

describes the dipole–dipole interaction between molecules where $J^{gege}_{mn} = J^{*gege}_{nm}$. The first term on the right-hand-side of Eq. (6) describes the excitation of molecule m and deexcitation of molecule n, and the second term describes a similar effect but with the replacement of m by n and vice versa.

3. Evolution of wave function

3.1. Evolution of wave function related to the processes of exciton–exciton annihilation

Consider first the evolution of the two-exciton wave function under the exciton–exciton annihilation processes

$$i\hbar\frac{d\Psi}{dt} \propto (H_0 + H_{annih})\Psi \quad (7)$$

Substituting Eq. (2) into Eq. (7) and using Eqs. (5) and (1), we get equations for the amplitudes C_{mn} and $d_{m\nu}$ $(m > n)$

$$i\hbar\frac{dC_{mn}}{dt} = \hbar(\omega_{me,g} + \omega_{ne,g})C_{mn} + \sum_{\nu}(d_{m\nu}V_{mn} + d_{n\nu}V_{nm})$$

$$i\hbar\frac{dd_{m\nu}}{dt} = \hbar\omega_{mf\nu,g}d_{m\nu} + \sum_{m>n}C_{mn}V_{nm} + \sum_{n>m}C_{nm}V_{nm} \quad (8)$$

Eq. (8) may be written in more symmetric form by introducing a new function

$$Q_{mn} = \begin{Bmatrix} C_{mn} & m > n \\ C_{nm} & n > m \end{Bmatrix} \quad (9)$$

that is symmetric with respect to indices m and n

$$i\hbar\frac{dQ_{mn}}{dt} = 2\hbar\omega_{eg}Q_{mn} + \sum_{\nu}(d_{m\nu}V_{mn} + d_{n\nu}V_{nm})$$

$$i\hbar\frac{dd_{m\nu}}{dt} = \hbar\omega_{f\nu g}d_{m\nu} + \sum_{m\neq n}Q_{mn}V_{nm} \quad (10)$$

where we put $\omega_{me,g} = \omega_{eg}$ and $\omega_{mf\nu,g} = \omega_{f\nu g}$ (the ensemble of identical molecules). To solve Eq. (10), let us introduce slowly changing variables q_{mn} and $p_{m\nu}$ using

$$Q_{mn} = q_{mn}\exp(-i2\omega_{eg}t)$$
$$d_{m\nu} = p_{m\nu}\exp(-i\omega_{f\nu g}t) \quad (11)$$

Then Eq. (10) can be written as

$$i\hbar\frac{dq_{mn}}{dt} = \sum_{\nu}z_{mn\nu}\exp(-i\Delta_{\nu}t)$$

$$i\hbar\frac{dz_{mn\nu}}{dt} = \exp(i\Delta_{\nu}t)\left(\sum_{k\neq m}q_{mk}V_{km}V_{mn} + \sum_{k\neq n}q_{nk}V_{kn}V_{nm}\right) - i\hbar\gamma z_{mn\nu} \quad (12)$$

where $\Delta_{\nu} = (\omega_{f\nu g} - 2\omega_{eg})$, and we denoted $p_{m\nu}V_{mn} + p_{n\nu}V_{nm} = z_{mn\nu}$ and took the decay γ of upper states $f\nu$ into account that includes vibrational relaxation. Formally integrating the second Eq. (12) and substituting the result into the first Eq. (12), we get

$$\frac{dq_{mn}}{dt} = -\frac{1}{\hbar^2}\sum_{\nu}\int_{-\infty}^{t}dt'\left(\sum_{k\neq m}q_{mk}(t')V_{km}V_{mn} + \sum_{k\neq n}q_{nk}(t')\times V_{kn}V_{nm}\right) \times\exp[-(\gamma + i\Delta_{\nu})(t-t')] \quad (13)$$

This results in a set of integro-differential equations for q_{mn}. The dynamics contains memory effects and is therefore non-Markovian. Next, we make a Markovian approximation by assuming that slowly varying functions $q_{mk}(t')$ can be moved as $q_{mk}(t)$ to outside the integral. Eq. (13) then becomes

$$\frac{dq_{mn}}{dt} = -\frac{1}{2}\left\{(w_{mn} - i4\Delta_{mnnm})q_{mn} + \sum_{k\neq m,n}[(\Gamma_{kmmn} - i2\Delta_{kmmn})q_{mk} + (\Gamma_{knnm} - i2\Delta_{knnm})q_{nk}]\right\} \quad (14)$$

where $w_{mn} = 2\Gamma_{mnnm}$ is the exciton–exciton annihilation rate,

$$\Gamma_{kmmn} = \frac{2}{\hbar^2}V_{km}V_{mn}\sum_{\nu}\frac{\gamma}{\gamma^2 + \Delta_{\nu}^2} \quad (15)$$

and

$$\Delta_{kmmn} = \frac{1}{\hbar^2}V_{km}V_{mn}\sum_{\nu}\frac{\Delta_{\nu}}{\gamma^2 + \Delta_{\nu}^2} \quad (16)$$

that gives

$$\Gamma_{kmmn} = \frac{2\pi}{\hbar^2}V_{km}V_{mn}\sum_{\nu}\delta(\omega_{f\nu g} - 2\omega_{eg}) \quad (17)$$

and

$$\Delta_{kmmn} = \frac{1}{\hbar^2}V_{km}V_{mn}P\sum_{\nu}\frac{1}{\omega_{f\nu g} - 2\omega_{eg}} \quad (18)$$

in the limit $\gamma \to 0$. Here P denotes the principal value. Parameters Γ_{kmmn} and Γ_{knnm} on the right-hand side of Eq. (14) for $k \neq m, n$ are non-diagonal elements of the relaxation matrix relating the decay of two-exciton state $|mn>$ to those of two-exciton states $|mk>$ and $|nk>$, respectively. In that case they speak about interference effects in relaxation [22–24]. By this means the relaxation of two-exciton state is determined by non-diagonal relaxation matrix including contributions of both two- and three-particle processes. All these multiparticle relaxation terms have the interference nature, which reflects the fact that a transition to a given state can, as a rule, be realized not by only one pathway, but, rather, by a combination of different pathways. The interference relaxation parameter Γ_{kmmn} for $k = m-1$ and $n = m+1$ (interaction between nearest neighbors (see below)), $\Gamma_{(m-1)mm(m+1)} \sim V_{(m-1)m}V_{m(m+1)}$, is illustrated in Fig. 1.

In the approximation of the interaction between nearest neighbors and real V_{mn} when $V_{mn} = 0$ for $|m-n| > 1$, and $V_{mn} = V$ for $n = m \pm 1$, Eq. (14) becomes

$$\frac{dq_{m,m\pm1}}{dt} = -(\alpha - i2\beta)\left[q_{m,m\pm1} + \frac{1}{2}(q_{m,m\mp1} + q_{m\pm1,m\pm2})\right] \quad (19)$$

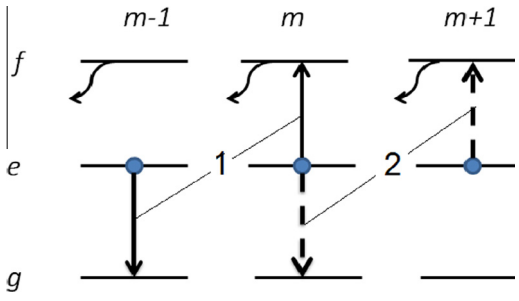

Fig. 1. Scheme of the interference processes in the exciton–exciton annihilation described by $\Gamma_{(m-1)mm(m+1)} \sim V_{(m-1)m}V_{m(m+1)}$, according to which two-exciton state with wave function $\Psi \sim C_{m(m-1)}|me(m-1)e\rangle\prod_{k\neq m,m-1}|kg\rangle + C_{(m+1)m}|(m+1)eme\rangle\prod_{k\neq m+1,m}|kg\rangle$, Eq. (2), can decay due to the interference of processes 1 and 2 shown by solid and dashed arrow, respectively. In the process 1, the molecule $m-1$ goes to the ground state while the molecule m passes to the third level. In the process 2, the molecule m goes to the ground state while the molecule $m+1$ passes to the third level. This is a three-particle process. The next step is the radiationless relaxation of the third level (shown by wave arrows).

where

$$\alpha = \frac{2V^2}{\hbar^2}\sum_v \frac{\gamma}{\gamma^2+\Delta_v^2} = \frac{2\pi V^2}{\hbar^2}\sum_v \delta(\omega_{fvg}-2\omega_{eg}) \tag{20}$$

$$\beta = \frac{V^2}{\hbar^2}\sum_v \frac{\Delta_v}{\gamma^2+\Delta_v^2} = \frac{V^2}{\hbar^2}P\sum_v \frac{1}{\omega_{fvg}-2\omega_{eg}} \tag{21}$$

Below we shall generalize Eq. (19) to the presence of the dipole–dipole interactions described by Hamiltonian H_{int} , Eq. (6). Exact solution of Eq. (19) is given in Appendix A where we neglected β-terms in comparison with the α-terms.

3.2. Evolution of wave function in the presence of the dipole–dipole interactions described by Hamiltonian H_{int}

Consider now evolution of the two-exciton wave function under the influence of H_{int}

$$i\hbar\frac{d\Psi}{dt} \propto H_{int}\Psi \tag{22}$$

Substituting Eq. (2) into Eq. (22) and using Eq. (6), we get equations for the amplitudes C_{mn} $(m>n)$ after cumbersome algebraic rearrangements.

$$\frac{i}{2}\frac{dC_{mn}}{dt} \propto \sum_{\substack{k>n,\\ k\neq m}} J^{gege}_{mk}C_{kn} + \sum_{\substack{n>k,\\ k\neq m}} J^{gege}_{mk}C_{nk} + \sum_{\substack{m>k,\\ k\neq n}} J^{gege}_{nk}C_{mk} + \sum_{\substack{k>m,\\ k\neq n}} J^{gege}_{nk}C_{km} \tag{23}$$

In the case of a nearest-neighbor interaction, an exact solution of Eq. (23) may be obtained by transforming the Paulion operators $(B_m^{\dagger}, B_n)$ in Hamiltonian H_{int} to fermion operators through the Jordan–Wigner transformation [25–28]. Then eigenvalues of energy and eigenfunctions for a single-exciton excitation are given by

$$E_\mu = \hbar\omega_{eg} + 2\hbar J\cos\left(\frac{\pi\mu}{N+1}\right) \tag{24}$$

and

$$|\mu\rangle = \sqrt{\frac{2}{N+1}}\sum_{n=1}^{N}\sin\left(\frac{\pi n\mu}{N+1}\right)|ne\rangle \tag{25}$$

where $J \equiv J^{gege}_{mm\pm1}$; $\mu = 1,\ldots N$; N is the number of molecular sites in a J-aggregates. Eigenvalues of energy and eigenfunctions for a two-exciton excitations are given by

$$E_{\mu\nu} = 2\hbar\omega_{eg} + 2\hbar J\left[\cos\left(\frac{\pi\mu}{N+1}\right) + \cos\left(\frac{\pi\nu}{N+1}\right)\right] \tag{26}$$

$$|\mu\nu\rangle = \sum_{m>n} U_{\mu\nu,mn}|mene\rangle \tag{27}$$

where $1 \leqslant \nu < \mu \leqslant N$, and the matrix $U_{\mu\nu,mn}$ is determined as

$$U_{\mu\nu,mn} = \frac{2}{N+1}\left[\sin\left(\frac{\pi\mu m}{N+1}\right)\sin\left(\frac{\pi\nu n}{N+1}\right) - \sin\left(\frac{\pi\mu n}{N+1}\right)\sin\left(\frac{\pi\nu m}{N+1}\right)\right] \tag{28}$$

The total evolution of amplitudes C_{mn}, Eq. (8), under the influence of both H_{int} and the exciton–exciton annihilation processes, Eq. (19), in the case of a nearest-neighbor interaction is given by

$$\begin{aligned}\frac{dC_{mn}}{dt} &= -\frac{i}{\hbar}\sum_{m'>n'}(H_{eff})_{mnm'n'}C_{m'n'} \\ &= -i2\omega_{eg}C_{mn} - \frac{i}{\hbar}\sum_{m'>n'}(H_{int})_{mnm'n'}\delta_{n,m-1}C_{m'n'} \\ &\quad - \alpha\left(C_{mm-1} + \frac{1}{2}C_{m+1m} + \frac{1}{2}C_{m-1m-2}\right)\end{aligned} \tag{29}$$

for $m>n$ where we neglected β-terms in comparison with the α-terms. Here we have introduced an effective Hamiltonian H_{eff}

$$(H_{eff})_{mnm'n'} = 2\hbar\omega_{eg}\delta_{mm'}\delta_{nn'} + (H_{int})_{mnm'n'}\delta_{n,m-1} - i\hbar\alpha(V_{ex-ex})_{mn,m'n'} \tag{30}$$

that will be diagonalized below. Here $m>n, m'>n'$ and

$$(V_{ex-ex})_{mn,m'n'} = \delta_{n,m-1}\left(\delta_{nn'}\delta_{mm'} + \frac{1}{2}\delta_{m',m+1}\delta_{n'm} + \frac{1}{2}\delta_{m',m-1}\delta_{n',m-2}\right) \tag{31}$$

Next let us pass on to the basis of two-exciton states $|\mu\nu\rangle$ from the site basis bearing in mind that

$$\sum_{m>n} C_{mn}|mene\rangle = \sum_{\mu>\nu} T_{\mu\nu}|\mu\nu\rangle \tag{32}$$

Using Eq. (27), we get

$$C_{mn} = \sum_{\mu>\nu} U_{\mu\nu,mn}T_{\mu\nu},\ m>n$$

where $U_{\mu\nu,mn}$ is an unitary real matrix. Then the inverse matrix is equal to the transposed matrix, i.e. $U^{-1} = U^T$, and $U_{\mu\nu,mn} = U_{mn,\mu\nu}$. This gives

$$T_{\mu\nu} = \sum_{m>n} U_{\mu\nu,mn}C_{mn} \tag{33}$$

for $\mu>\nu$. Using Eqs. (29) and (33), one gets

$$i\hbar\frac{dT_{\mu\nu}}{dt} = \sum_{\mu'>\nu'}\sum_{m>n}\sum_{m'>n'}(H_{eff})_{mnm'n'}U_{\mu\nu,mn}U_{\mu'\nu',m'n'}T_{\mu'\nu'} \tag{34}$$

where $\mu>\nu$. The part of the effective Hamiltonian related to H_{int} is diagonal in the $|\mu\nu\rangle$ basis, and we obtain

$$\begin{aligned}i\hbar\frac{dT_{\mu\nu}}{dt} = \sum_{\mu'>\nu'}\Bigg\{&\hbar\left[2\omega_{eg} + 2J\left(\cos\left(\frac{\pi\mu}{N+1}\right) + \cos\left(\frac{\pi\nu}{N+1}\right)\right)\right] \\ &\times\delta_{\mu\mu'}\delta_{\nu\nu'} - i\hbar\alpha\sum_{m>n}\sum_{m'>n'}(V_{ex-ex})_{mn,m'n'}U_{\mu\nu,mn}U_{\mu'\nu',m'n'}T_{\mu'\nu'}\Bigg\}\end{aligned} \tag{35}$$

Let us calculate matrix elements V_{ex-ex} in the $|\mu\nu\rangle$ basis (see the last term in the curly brackets on the right-hand side of Eq. (35))

$$(V_{ex-ex})_{\mu\nu,\mu'\nu'} = \sum_{m>n}\sum_{m'>n'}(V_{ex-ex})_{mn,m'n'}U_{\mu\nu,mn}U_{\mu'\nu',m'n'} \tag{36}$$

Using Eq. (31), one gets

$$\begin{aligned}(V_{ex-ex})_{\mu\nu,\mu'\nu'} = &\sum_{m=2}^{N}U_{\mu\nu,mm-1}U_{\mu'\nu',mm-1} + \frac{1}{2}\sum_{m=2}^{N-1}U_{\mu\nu,mm-1}U_{\mu'\nu',m+1m} \\ &+ \frac{1}{2}\sum_{m=3}^{N}U_{\mu\nu,mm-1}U_{\mu'\nu',m-1m-2}\end{aligned} \tag{37}$$

Changing summation indices and using Eq. (28), we finally obtain after cumbersome algebraic rearrangements

$$\begin{aligned}\alpha(V_{ex-ex})_{\mu\nu,\mu'\nu'} = &Y(\mu,\nu,\mu',\nu') + Y(\mu,-\nu,\mu',-\nu') \\ &- Y(\mu,-\nu,\mu',\nu') - Y(\mu,\nu,\mu',-\nu')\end{aligned} \tag{38}$$

where function $Y(\mu,\nu,\mu',\nu')$ is defined as

$$\begin{aligned}Y(\mu,\nu,\mu',\nu') = &\frac{4\alpha}{(N+1)^2}\sin\frac{\pi(\mu-\nu)}{2(N+1)}\sin\frac{\pi(\mu'-\nu')}{2(N+1)}\times\cos\frac{\pi(\mu+\nu)}{2(N+1)} \\ &\times\cos\frac{\pi(\mu'+\nu')}{2(N+1)} \\ &\times\sum_{m=1}^{N}\left[\cos\frac{\pi(\mu+\nu-\mu'-\nu')m}{(N+1)} - \cos\frac{\pi(\mu+\nu+\mu'+\nu')m}{(N+1)}\right]\end{aligned} \tag{39}$$

Here

$$\sum_{m=1}^{N}\cos\left(\frac{\pi x m}{N+1}\right)=\left\{\begin{array}{c} N \text{ for } x=0 \text{ or } x=2l(N+1) \\ -1 \text{ for } x=2n \text{ where } n\neq l(N+1) \\ 0 \text{ for } x=2n+1 \end{array}\right\} \quad (40)$$

Eigenvalues for energy and decay of the two-exciton states can be found by diagonalization of the effective Hamiltonian, Eq. (30), that couples all the two-exciton states. This will be done numerically in the next section.

4. Eigenvalues for energy and decay of two-exciton states

Consider Eq. (31) for the imaginary part "$-\hbar\alpha(V_{ex-ex})_{mn,m'n'}$" of the effective Hamiltonian, Eq. (30),

$$-\hbar\alpha(V_{ex-ex})_{mn,m'n'}=-\hbar\alpha\left[(V_{ex-ex})_{m,m-1;m,m-1}+\frac{1}{2}(V_{ex-ex})_{m,m-1;m+1,m}+\frac{1}{2}(V_{ex-ex})_{m,m-1;m-1,m-2}\right] \quad (41)$$

where $m>n, m'>n'$. The first term on the right-hand side of Eq. (41) represents usual bimolecular decay of the two-exciton state. At the same time the second and the third terms are related to three-particle processes and are interference terms in nature. The point is that due to deactivation of molecule m both $m+1$ and $m-1$ excited molecules can pass to their third levels $|f\rangle$ destructing the two-exciton state.

4.1. Spectrum of two-exciton states

The eigenvalues of the non–Hermitian effective Hamiltonian are complex. Consider first their real parts defining the spectrum of the two-exciton states of a J-aggregate ($J<0$), Figs. 2–5, that are given in terms of relative quantity $\varepsilon=\frac{E-2\hbar\omega_{eg}}{\hbar|J|}$.

At first glance the figures show that the processes of the exciton–exciton annihilation not strongly affected the spectrum extending the plateau corresponding to zero values of ε. The spectrum is scarcely affected by the interference processes in the exciton–exciton annihilation. However, the eigenvalues of energy are markedly affected by the exciton–exciton annihilation processes (see Table 1). This effect rises as a number of state increases. The second, third and fourth columns of Table 1 represent the state energies in terms of cm^{-1} for the corresponding value of α and $|J|=600\ cm^{-1}$.

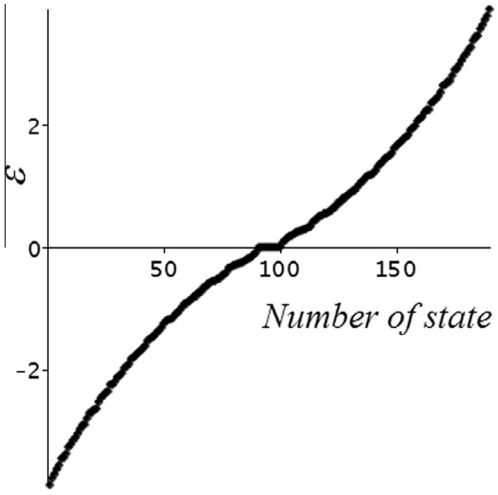

Fig. 2. Spectrum of two-exciton states in the absence of exciton–exciton annihilation ($\alpha=0$) for $N=20$.

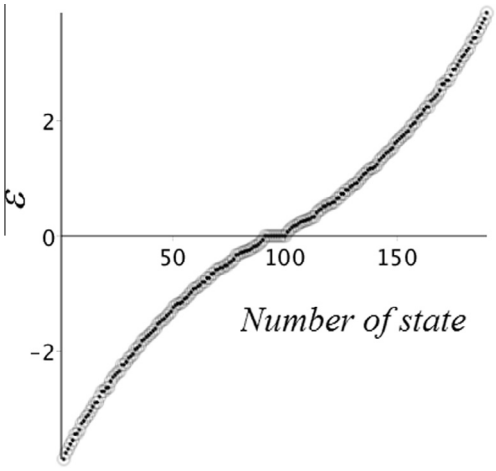

Fig. 3. Spectrum of two-exciton states for $N=20$ and $\alpha=-0.1$ J (solid diamonds). For comparison we also show spectrum without taking the interference processes in the exciton–exciton annihilation into account (see Appendix A) (open circles).

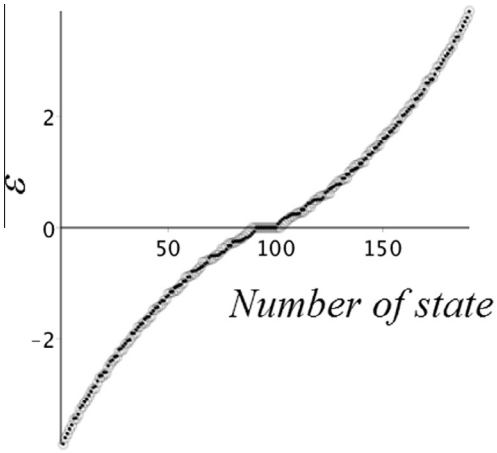

Fig. 4. Spectrum of two-exciton states for $N=20$ and $\alpha=-$J (solid diamonds). For comparison we also show spectrum without taking the interference processes in the exciton–exciton annihilation into account (open circles).

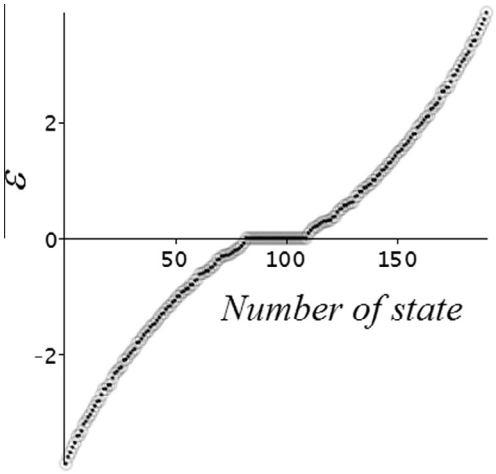

Fig. 5. Spectrum of two-exciton states for $N=20$ and $\alpha=-10$ J (solid diamonds). For comparison we also show spectrum without taking the interference processes in the exciton–exciton annihilation into account (open circles).

4.2. Decay of two-exciton states

Consider now the imaginary parts of the eigenvalues of the effective Hamiltonian defining the decay of the two-exciton states due to the exciton–exciton annihilation, Figs. 6–9, 10,11, that are given in terms of the relative quantity *decay*/|*J*|.

Figs. 6 and 7 show that for small α, taking the interference processes in the exciton–exciton annihilation into account increases the lifetime of the states with relative energy ε that is close to zero.

One can also see that for the states with relative energy ε that is close to zero, decay of a large number of states is large and is proportional to α. Taking the interference processes in the exciton–exciton annihilation into account increases the decay up to 2α, Fig. 10, that is associated with the signatures of the super-radiance [18]. The point is that the decay rate of this state (the decay of population) is 4α, i.e. twice the probability of bimolecular decay w_a that is equal to 2α.

However, there are also states with very large lifetimes in the region under consideration. In this case the contribution of the interference processes is very important. The decay is also suppressed for small and large ε. All the long-lived states under discussion are associated with the population trapping [21,18].

It is worthy to note that the influence of the interference processes in the exciton–exciton annihilation on lifetime depends on the value of α. The interference processes decrease the lifetime of lower and upper states for small α. For $\alpha > -2$ J, the interference processes increase lifetimes of the lower and upper states. For some values of α the interference processes contribution is small. Fig. 12 represents the decay of the lower state as a function of α that appears as a non-monotonous one. It is worthy to note that decays for very small and large α look much the same that is associated with the population trapping [21,18] for large α.

5. Comparison with previous results and experiment

Previously authors of earlier pioneering works [13,14] related the decay of the lowest state $|21\rangle$ from the two-exciton excited states $|\mu\nu\rangle$ to the probability of bimolecular decay w_a that is equal to 2α using our designations. Accordingly, their calculations correspond to the calculation of only the diagonal matrix element $\alpha(V_{ex-ex})_{\mu\nu,\mu'\nu'}$ for $\mu = \mu' = 2$ and $\nu = \nu' = 1$. Indeed, using Eqs. (38)–(40), one gets

Table 1
Real parts of the eigenvalues of the non–Hermitian effective Hamiltonian defining spectrum of two-exciton states.

State number	$\alpha = 0$	$\alpha = -$J	$\alpha = -10$ J
1	−2333.2	−2330.2	−2326.6
2	−2267.8	−2261.7	−2254.6
4	−2278.1	−2168.3	−2156.3
6	−2072.6	−2057.7	−2040.3
8	−2026.3	−2010.3	−1990.2
9	−1960.8	−1941.4	−1918.1
10	−1934.8	−1916.6	−1891.1
12	−1871.1	−1847.5	−1989.8
14	−1786.6	−1764.5	−1730.7
16	−1739.7	−1711.3	−1676.7
18	−1627.9	−1599.9	−1556.9
20	−1591.5	−1558.7	−1516.2
22	−1519.6	−1488.3	−1440.8
24	−1453.6	−1426.8	−1374.0
26	−1413.7	−1384.5	−1330.0
28	−1348.2	−1304.3	−1250.6
30	−1276.3	−1249.4	−1186.5
32	−1236.4	−1207.0	−1142.5
34	−1170.8	−1137.6	−1070.4
36	−1096.9	−1071.7	−999.0
38	−1057.0	−1029.4	−955.0
39	−1038.4	−984.8	−916.0
40	−1015.2	−965.0	−893.7

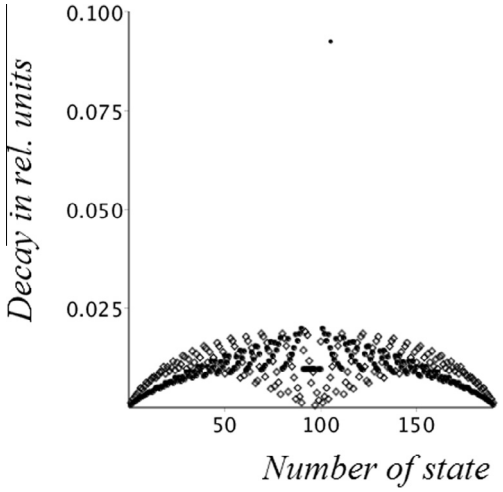

Fig. 6. Decay of two-exciton states for $N = 20$ and $\alpha = -0.1$ J (diamonds). For comparison we also show the decays without taking the interference processes in the exciton–exciton annihilation into account (see Appendix A) (solid circles).

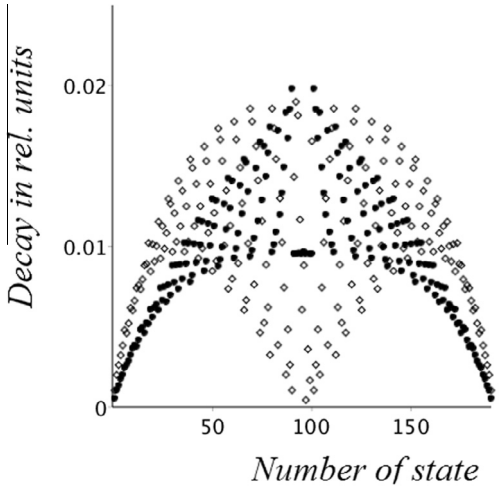

Fig. 7. The same as in Fig. 6 for small decay.

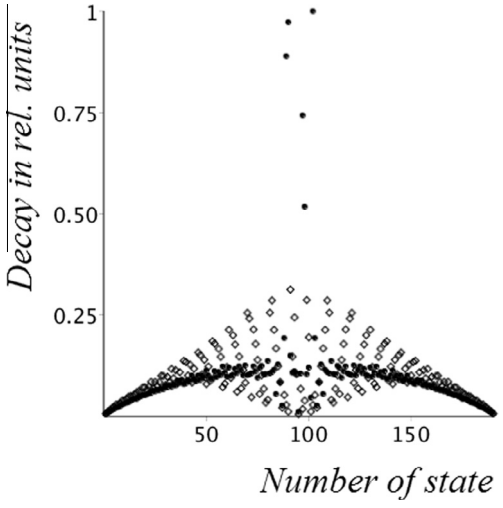

Fig. 8. Decay of two-exciton states for $N = 20$ and $\alpha = -$J (diamonds). For comparison we also show the decays without taking the interference processes in the exciton–exciton annihilation into account (see Appendix A) (solid circles).

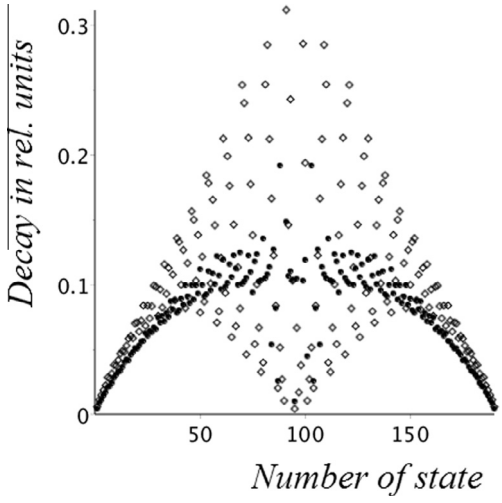

Fig. 9. The same as in Fig. 8 for small decay.

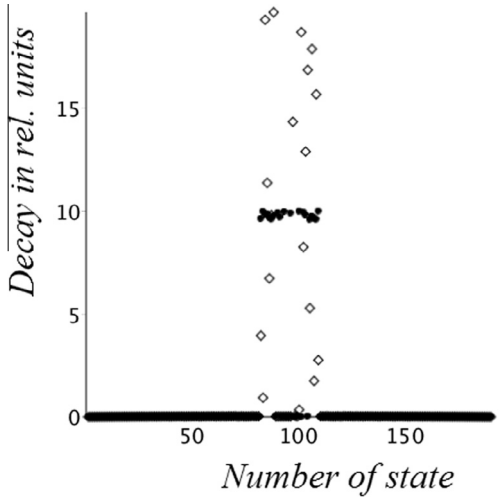

Fig. 10. Decay of two-exciton states for $N = 20$ and $\alpha = -10$ J (diamonds). For comparison we also show the decays without taking the interference processes in the exciton–exciton annihilation into account (see Appendix A) (solid circles).

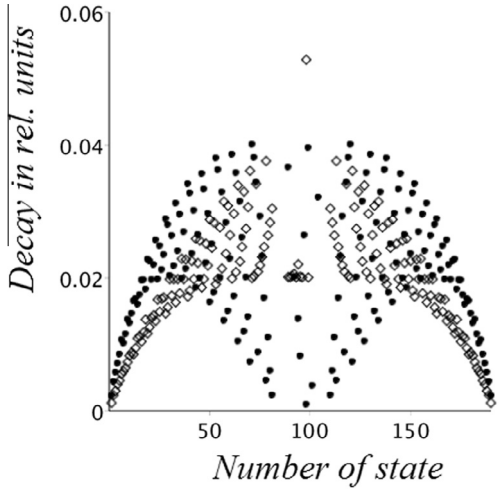

Fig. 11. The same as in Fig. 10 for small decay.

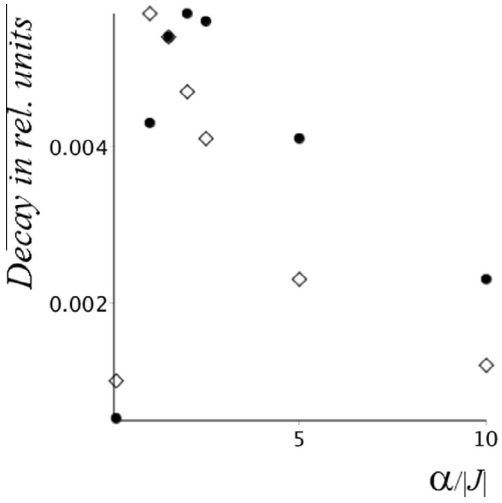

Fig. 12. Decay of the lower state of the two-exciton states as a function of α for $N = 20$ (diamonds). For comparison we also show decays without taking the interference processes in the exciton–exciton annihilation into account (solid circles).

$$\alpha(V_{ex-ex})_{21,21} = \frac{2\alpha}{N+1}\left(\sin^2\frac{2\pi}{N+1} + \sin^2\frac{\pi}{N+1}\right) \tag{42}$$

that is one half the exciton–exciton annihilation rate calculated in Eq. (8) of Ref. [13]. The last formula gives $\alpha(V_{ex-ex})_{21,21} \simeq 10\alpha\pi^2/N^3$ for $N \gg 1$ that is about $1.2 \times 10^{-2}\alpha$ for $N = 20$.

However, states $|\mu\nu\rangle$ are eigenstates of only the real part of the effective Hamiltonian, Eq. (30), with no regard for its imaginary part that is of order of α. As noted in the Introduction, if the width 2α is of the order of, or exceeds, the spacing between real energies E, this means the transition to the regime of overlapping resonances that supplies the system by the new collectivity - the possibility of coherent decay. So that one should compare α with the energy space between adjacent two-exciton states. Using the representation of $w_a = 2\alpha$ by formula (2) of Ref. [13], $w_a = 4\pi V^2/(\hbar^2\Gamma)$, one can evaluate α. In the latter formula the density of final states $\rho(E) = \sum_\nu \delta(E - E_{f\nu})$ was substituted by the inverse relaxation constant $(\hbar\Gamma)^{-1}$ (compare with Eq. (20)). We choose the value of $V \approx 600\ \mathrm{cm}^{-1}$ from Refs. [13,12,29]. Authors of Ref. [13] related Γ to the rate of vibrational relaxation of high-lying levels that can be evaluated as $10^{13} - 10^{14}\ \mathrm{s}^{-1}$ [30–32]. These values of parameters give us $\alpha = (678.6 \div 6786)\ \mathrm{cm}^{-1}$, i.e. $\alpha/V \sim 1 \div 10$. Such values of α not only exceed the energy space between adjacent two-exciton states, but can exceed all the range spanned by these states equal to $8|J| \sim 8V \approx 4800\ \mathrm{cm}^{-1}$ as well. This means the regime of overlapping resonances that supplies the system by the new collectivity - the possibility of coherent decay in the annihilation channel.

Since $\alpha/V \sim 1 \div 10$, we shall concentrate on Figs. 8, 9 and Figs. 10, 11 for $\alpha = -$J and $\alpha = -10$ J, respectively. The second and third columns of Table 2 represent the state decays in terms of cm^{-1} for the corresponding value of α and $J = -600\ \mathrm{cm}^{-1}$. The energies of the corresponding states are given in Table 1.

The third column of Table 2 shows that the state decays for $\alpha = -10$ J are very small demonstrating well-marked population trapping. In contrast, the second column of Table 2 corresponding to $\alpha = -$J, shows decays that are closer to experimental values of Ref. [12] that are related to the decay of $81\ \mathrm{cm}^{-1}$ for the fastest component. In addition, Fig. 12 demonstrates that the largest decays of lower states are realized just for $\alpha = -$J. So, the choice of relation $\alpha = -$J seems us more reasonable. In addition, an

inequality, $\Gamma > V$, is needed for using the perturbation theory to calculate the bimolecular rate of the exciton–exciton annihilation, w_a [13], and also α. This inequality is realized for $\Gamma = 10^{14}$ s^{-1} that gives $\alpha = -$J, and is not realized for $\Gamma = 10^{13}$ s^{-1} that gives $\alpha = -10$ J.

Let us compare the decays of the second column of Table 2 with experiment [12]. They observed a number of decay components from which at least three exponential functions with the characteristic time constants of 200 fs, 1.5 ps, and 20 ps were needed. It is worthy to note that relaxation of high vibrational states of large molecules in solutions occurs in two steps [30–32]. The first step is very fast intramolecular relaxation with the characteristic time of $10^{-13} - 10^{-14}$ s that increases an intramolecular temperature. The next step is cooling "hot" molecules till the temperature of the surrounding due to intermolecular relaxation that occurs during $\sim 10^{-11}$ s. So, we relate the decay of 20 ps with cooling the excited molecules (see also [11] where cooling with the characteristic time of 18 ps was observed in excitonic systems). As to concerns the intermediate decay of 1.5 ps, it corresponds to the decay constant of 11.1 cm^{-1} that is realized for the state number 4 (see the second column of Table 2). The energy of state 4 is higher than that of state 1 for 162 cm^{-1} (see the third column of Table 1). The photon of $\lambda = 570$ nm with energy of 17546 cm^{-1} used in experiment [12] can lead to heating the high vibrationally excited molecule created due to the exciton–exciton annihilation process for $\Delta T = 17546\ \text{cm}^{-1}/C_{vib} \simeq 244$ K where the vibrational heat capacity $C_{vib} \sim 50$ cm^{-1} K^{-1} was used [30] that is characteristic for large molecules. Bearing in mind the temperature of the surrounding of 20 K in experiment [12], one gets the temperature of the high vibrationally excited molecule as $T^* \simeq 264$ K that leads to the excess energy of 380 cm^{-1} covering states up to 9–10 (see the third column of Table 1). As a matter of fact, the decay constant of 11.1 cm^{-1} may be considered as an averaged decay constant of the states populated at temperature T^*. This is a new option for the explanation of the intermediate decay of 1.5 ps that was related before to the annihilation of two excitons created within separated localization segments [12].

Furthermore, the fastest component of decay of 200 fs observed in experiment [12] corresponds to the decay of state 39, the second column of Table 2. The energy of this state is higher than that of the lowest state for 1345 cm^{-1}. In principle, the state with the excess energy of about 1345 cm^{-1} may be excited by direct optical transition from the single-exciton state. Let us evaluate the corresponding dipole moment. A uniform excitation by an external electric field with a wave vector oriented normal to the aggregate axis excites only the single-exciton $k = 0$ state with energy $\hbar\omega_{eg} + 2\hbar$ J [16]. Then the exciton-qth-biexciton transition dipole moment from this state is proportional to $\cot[\pi q/(2N)]$ where the energy of the q th-biexciton state is given by $2\hbar\omega_{eg} + 4\hbar J\cos(\pi q/N)$ [33,16]. Here $q = 1, 3, 5, \ldots, N^*$, where $N^* = N - 2$ for N odd and $N^* = N - 1$ for N even. The state with the excess energy of 1345 cm^{-1} corresponds to $q \approx 7$ that gives for the ratio between the dipole moments for the transitions to the 7th- and first biexciton states $\cot[7\pi/(2N)]/\cot[\pi/(2N)] \simeq 0.13$. It is well to bear in mind that this evaluation is based on only the real part of the effective Hamiltonian with no regard for its imaginary part. Calculations of the dipole moments based on the eigenstates of the effective Hamiltonian are beyond the scope of our present work.

Unfortunately, the authors of Ref. [12] did not provide the whole set of experimental data relative to the kinetics of the exciton–exciton annihilation except that at least three exponential functions were needed (see above) with no indications of their weights. In addition, they related the fastest component of decay of 200 fs to the decay time of the $n(\geqslant 2)$-exciton states, from which only two-exciton states were considered in our work. It is worthy to note in this connection that if the biexcitonic state with the excess energy of about 1345 cm^{-1} is excited, its decay due to the exciton–exciton annihilation will be accompanied by the vibrational relaxation with the rate of $10^{12} - 10^{13}$ s^{-1} that is slower than that of high excited vibrational states (see above). So, the 200 fs component of the exciton–exciton annihilation is quite competitive with the vibrational relaxation, and may manifest itself in experiment.

It is worthy to note that in the present work we calculated the rate of the exciton–exciton annihilation using the nearest-neighbor approximation. However, the coupling to far neighbors gives rise to increase of the intrasegment annihilation rate by a factor of 2.7 [14]. In such a case, already the state number 12 will decay with the rate of the fastest component (see Table 2). State 12 corresponds to the excess energy of only 483 cm^{-1} (see Table 1) that allows to populate it due to increasing an intramolecular temperature or by direct optical transition from the single-exciton state

Table 2
Imaginary parts of the eigenvalues of the non–Hermitian effective Hamiltonian defining decay of two-exciton states.

State number	$\alpha = -$J	$\alpha = -10$ J
1	3.4	0.7
2	6.7	1.4
3	8.8	1.8
4	11.1	2.4
6	17.1	3.3
8	18.9	3.9
10	22.6	5
12	28.1	5.1
14	29.0	6.6
16	35.0	6.3
18	35.3	8.3
20	42.6	7.5
22	43.4	8.6
24	41.0	10
26	44.4	10.1
28	59.6	8.8
30	45.66	11.9
32	49.49	11.9
34	55.9	11.9
36	48.6	13.7
38	52.4	13.7
39	81.6	10.3
40	79.9	10.9

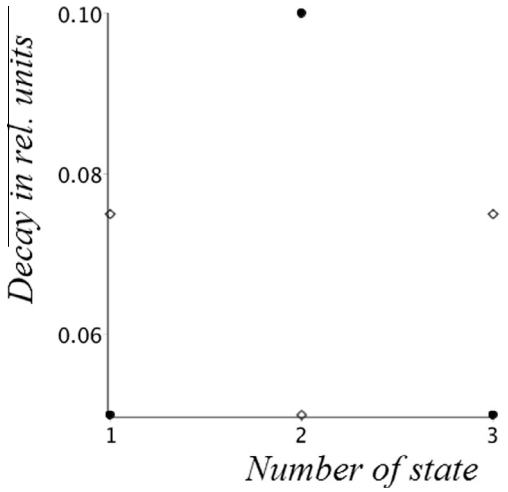

Fig. 13. Decay of two-exciton states for $N = 3$ and $\alpha = -0.1$ J (diamonds). For comparison we also show the decays without taking the interference processes in the exciton–exciton annihilation into account (see Appendix A) (solid circles).

to $q \approx 3 \div 5$ (see above). The values $q = 3$ and $q = 5$ give for the ratio between the dipole moments for the transitions to the qth and first biexciton states $\cot[3\pi/(2N)]/\cot[\pi/(2N)] \simeq 0.33$ and $\cot[5\pi/(2N)]/\cot[\pi/(2N)] \simeq 0.2$, respectively. This issue will be considered in more detail elsewhere.

6. Conclusion

In this work we have studied the decay of the two-exciton excited states of a J-aggregate that is collective in nature. The collective character of the decay is due to both the dipole–dipole interaction between molecules and the interference processes in the exciton–exciton annihilation [17]. It is well known that the collective states can demonstrate various behaviors, the two extreme cases of which are super-radiance by Dicke [19,20] and the population trapping [21,18]. For the description of the corresponding physics in this work we used the mathematical formalism based on the effective non–Hermitian Hamiltonian [18] suggested in nuclear theory. Our calculations show that the processes of the exciton–exciton annihilation affected the spectrum extending the plateau corresponding to zero values of the relative energy ε. In addition, the spectrum is scarcely affected by the interference processes in the exciton–exciton annihilation. However, the eigenvalues of energy are markedly affected by the exciton–exciton annihilation processes (see Table 1). This effect rises as a number of state increases.

In contrast, the decay of the two-exciton states is strongly affected by the interference processes. For small bimolecular decay rates, α, taking the interference processes in the exciton–exciton annihilation into account increases the lifetime of the states with relative energies ε that are close to zero. For the same region of states, decay of a number of states is large and is proportional to α. Taking the interference processes in the exciton–exciton annihilation into account increases the decay up to 2α that is associated with the signatures of the super-radiance [18]. However, there are also states with very large lifetimes in the region under consideration. In this case the contribution of the interference processes is very important. The decay is also suppressed for small and large ε. All the long-lived states under discussion are associated with the population trapping [21,18].

The influence of the interference processes in the exciton–exciton annihilation on lifetime depends on the relation between α and J. The interference processes decrease the lifetime of lower and upper states for small α. For $\alpha > -2$ J, the interference processes increase lifetimes of the lower and upper states. For some values of α the interference processes contribution is small. In addition, comparing Fig. 13 with the figures of Section 4.2, one can readily see that the smaller is the number of molecules in the aggregate, the greater is the influence of the interference processes in the exciton–exciton annihilation on the distribution of the decay values throughout the energy spectrum.

We have compared our approach with previous results [13] based on the eigenstates of only the real part of the effective Hamiltonian with no regard for its imaginary part. Our evaluations of the imaginary part show that it exceeds the spacing between real energies of the two-exciton states that gives rise to the transition to the regime of overlapping resonances supplying the system by the new collectivity - the possibility of coherent decay in the annihilation channel. We have also considered experiment [12] in the framework of our approach, the picture of which appears to be more complex and richer than it was reasoned before.

The results of the paper can be used for planning nonlinear optical experiments with J-aggregates, in order to avoid strongly decaying two-exciton states and involve in the main long-lived states associated with the population trapping.

Conflict of interest

There is no conflict of interest among authors.

7. Acknowledgments

We gratefully acknowledge support by the Russian–Israeli grant for Nanotechnology (No. 35803), and the US–Israel Binational Science Foundation (BF, Grant No. 2008282).

Appendix A

Since one of the aims of this work is the investigation of the role of the multiparticle interference processes in the exciton–exciton annihilation predicted in Ref. [17], we shall also consider matrix elements V_{ex-ex} without taking the interference processes into account

$$(V_{ex-ex})'_{\mu\nu,\mu'\nu'} = \frac{1}{2}\sum_{m=1}^{N-1} U_{\mu\nu,m+1m}U_{\mu'\nu',m+1m} + \frac{1}{2}\sum_{m=2}^{N} U_{\mu\nu,mm-1}U_{\mu'\nu',mm-1} \tag{43}$$

where

$$\begin{aligned}\alpha(V_{ex-ex})'_{\mu\nu,\mu'\nu'} &= Y'(\mu,\nu,\mu',\nu') + Y'(\mu,-\nu,\mu',-\nu') \\ &\quad - Y'(\mu,-\nu,\mu',\nu') - Y'(\mu,\nu,\mu',-\nu')\end{aligned} \tag{44}$$

and function $Y'(\mu,\nu,\mu',\nu')$ is determined as

$$\begin{aligned}Y'(\mu,\nu,\mu',\nu') &= \frac{2\alpha}{(N+1)^2}\sin\frac{\pi(\mu-\nu)}{2(N+1)}\sin\frac{\pi(\mu'-\nu')}{2(N+1)} \\ &\quad\times\left[\cos\frac{\pi(\mu+\nu-\mu'-\nu')}{2(N+1)}\sum_{m=1}^{N}\cos\frac{\pi(\mu+\nu-\mu'-\nu')m}{(N+1)}\right. \\ &\quad\left.-\cos\frac{\pi(\mu+\nu+\mu'+\nu')}{(N+1)}\sum_{m=1}^{N}\cos\frac{\pi(\mu+\nu+\mu'+\nu')m}{(N+1)}\right]\end{aligned} \tag{45}$$

One can also separate out the contribution of the interference terms

$$\begin{aligned}\alpha(V_{ex-ex})^{int}_{\mu\nu,\mu'\nu'} &= Y^{int}(\mu,\nu,\mu',\nu') + Y^{int}(\mu,-\nu,\mu',-\nu') \\ &\quad - Y^{int}(\mu,-\nu,\mu',\nu') - Y^{int}(\mu,\nu,\mu',-\nu')\end{aligned} \tag{46}$$

where

$$\begin{aligned}Y^{int}(\mu,\nu,\mu',\nu') &= \frac{2\alpha}{(N+1)^2}\sin\frac{\pi(\mu-\nu)}{2(N+1)}\sin\frac{\pi(\mu'-\nu')}{2(N+1)} \\ &\quad\times\left[\cos\frac{\pi(\mu+\nu+\mu'+\nu')}{2(N+1)}\sum_{m=1}^{N}\cos\frac{\pi(\mu+\nu-\mu'-\nu')m}{(N+1)}\right. \\ &\quad\left.-\cos\frac{\pi(\mu+\nu-\mu'-\nu')}{(N+1)}\sum_{m=1}^{N}\cos\frac{\pi(\mu+\nu+\mu'+\nu')m}{(N+1)}\right]\end{aligned} \tag{47}$$

It is easily seen that

$$\alpha(V_{ex-ex})_{\mu\nu,\mu'\nu'} = \alpha(V_{ex-ex})'_{\mu\nu,\mu'\nu'} + \alpha(V_{ex-ex})^{int}_{\mu\nu,\mu'\nu'} \tag{48}$$

Appendix B

Consider the evolution of the two-exciton wave function only under the exciton–exciton annihilation processes in the approximation of the interaction between nearest neighbors, Eq. (19). Denoting $r_m = q_{m,m+1}$ and introducing new variable $t' = (\alpha - i2\beta)t$, we get

$$\frac{dr_m}{dt'} = -\left[r_m + \frac{1}{2}(r_{m-1} + r_{m+1})\right] \equiv -\sum_{k=1}^{N}\Lambda_{mk}r_k \tag{49}$$

The solution of Eq. (49) may be written as $[r_m] = \exp(-\Lambda t')[r_m(t'=0)]$ where matrix $\Lambda \equiv [\Lambda_{mk}]$ is a three-diagonal matrix with eigenvalues [34].

$$\lambda_k = 1 + \cos\frac{\pi k}{N} \tag{50}$$

and $k = 1, \ldots, N-1$. So, state k decays as $\propto \exp[-(1+\cos\frac{\pi k}{N})(\alpha - i2\beta)t]$. Specifically, state $k = N-1$ is a long-lived state with lifetime $\tau_{N-1} = 1/\left[\alpha\left(1+\cos\frac{\pi(N-1)}{N}\right)\right] = 1/\left(\alpha 2\sin^2\frac{\pi}{2N}\right)$ that gives $\tau_{N-1} \simeq 2N^2/(\pi^2\alpha)$ for $N \gg 1$. This long-lived state is associated with the population trapping [18,21]. In contrast, state $k = 1$ has lifetime $\tau_1 = 1/[\alpha(1+\cos\frac{\pi}{N})]$ that gives $\tau_1 \simeq 1/(2\alpha)$ for $N \gg 1$. This lifetime is one-half that obtained without taking the interference processes in the exciton–exciton annihilation into account. It is worthy to note that short lifetime $\tau_1 \simeq 1/(2\alpha)$ correlates with the lifetime obtained numerically by diagonalization of the effective Hamiltonian in Section 4.2 for $\alpha = -10$ J, Fig. 10. One can appreciate the meaning of this, since the case under consideration in Appendix B corresponds to $\alpha \gg |J|$.

Appendix C

A simplest system that enables us to consider the interference processes in the exciton–exciton annihilation is a trimer, $N = 3$. A trimer has three two-exciton states with relative energies $\varepsilon = \frac{E-2\hbar\omega_0}{\hbar|J|}$ equal to $\varepsilon_1 = -\sqrt{2}$ for $\mu = 2$ and $\nu = 1, \varepsilon_2 = 0$ for $\mu = 3$ and $\nu = 1$, and $\varepsilon_3 = \sqrt{2}$ for $\mu = 3$ and $\nu = 2$. Using Eqs. (38) and (39) for $\mu = 2, 3$ and $\nu = 1, 2$ where $\mu > \nu$, one can calculate the matrix elements $\alpha(V_{ex-ex})_{\mu\nu,\mu'\nu'}$ of the effective Hamiltonian for the trimer that gives

$$\widetilde{H}_{eff} = \begin{pmatrix} -\sqrt{2} + i\frac{3\tilde{\alpha}}{4} & 0 & i\frac{\tilde{\alpha}}{4} \\ 0 & i\frac{\tilde{\alpha}}{2} & 0 \\ i\frac{3\tilde{\alpha}}{4} & 0 & \sqrt{2} + i\frac{3\tilde{\alpha}}{4} \end{pmatrix} \tag{51}$$

where $\widetilde{H}_{eff} \equiv (H_{eff} - 2\hbar\omega_0)/(\hbar|J|), \tilde{\alpha} \equiv \alpha/|J|$. The eigenvalues of $\widetilde{H}_{eff}$ can be found as the solutions of the equation $\det(\widetilde{H}_{eff} - \lambda E) = 0$. One gets $\lambda_2 = i\frac{\tilde{\alpha}}{2}, \lambda_{1,3} = i\frac{3\tilde{\alpha}}{4} \mp \sqrt{2 - \left(\frac{9\tilde{\alpha}^2}{16}\right)}$. It is easy to see that all the roots become imaginary for $\tilde{\alpha} > 4\sqrt{2}/3$. It is worthy to note that the same solution may be obtained for a trimer in the site representation combining Eqs. (19) and (23).

Fig. 13 shows the decays of the two-exciton states for a trimer. Comparing Fig. 13 with the figures of Section 4.2, one can readily see that the smaller is the number of molecules in the aggregate, the greater is the influence of the interference processes in the exciton–exciton annihilation on the distribution of the decay values throughout the energy spectrum.

References

[1] F.C. Spano, J. Knoester, Adv. Magn. Opt. Res. 18 (1994) 117.
[2] V.A. Malyshev, P. Moreno, Phys. Rev. A 53 (1) (1996) 416.
[3] H. Glaeske, V.A. Malyshev, K.H. Feller, Phys. Rev. A 65 (3) (2002). 033821 (10).
[4] A.S. Kiselev, A.S. Kiselev, N.N. Rozanov, JETP Lett. 87 (12) (2008) 663.
[5] N.V. Vysotina, V.A. Malyshev, V.G. Maslov, L.A. Nesterov, N.N. Rosanov, S.V. Fedorov, A.N. Shatsev, Opt. Spectrosc. 109 (1) (2010) 112 (Opt. Spektrosk. 109 (2010) 117).
[6] A. Suna, Phys. Rev. B 1 (4) (1970) 1716.
[7] V.M. Kenkre, Phys. Rev. B 22 (4) (1980) 2089.
[8] T. Renger, V. May, O. Kuhn, Phys. Rep. 343 (2001) 137.
[9] B. Bruggemann, V. May, J. Chem. Phys. 118 (2) (2003) 746.
[10] V. Sundstrom, T. Gillbro, R.A. Gadonas, A. Piskarskas, J. Chem. Phys. 89 (5) (1988) 2754.
[11] R. Gagel, R. Gadonas, A. Laubereau, Chem. Phys. Lett. 217 (3) (1994) 228.
[12] K. Minoshima, M. Taiji, K. Misawa, T. Kobayashi, Chem. Phys. Lett. 218 (1994) 67.
[13] V.A. Malyshev, H. Glaeske, K.H. Feller, Chem. Phys. Lett. 305 (1999) 117.
[14] V.A. Malyshev, G.G. Kozlov, H. Glaeske, K.H. Feller, Chem. Phys. 254 (2000) 31.
[15] T. Renger, V. May, V. Sundstrom, O. Kuhn, J. Chin. Chem. Soc. 47 (2000) 807.
[16] S. Mukamel, Principles of Nonlinear Optical Spectroscopy, Oxford University Press, New York, 1995.
[17] B.N. Levinsky, L.A. Nesterov, B.D. Fainberg, N.N. Rosanov, Opt. Spectrosc. 115 (3) (2013) 464.
[18] N. Auerbach, V. Zelevinsky, Rep. Prog. Phys. 74 (2011) 106301.
[19] R.H. Dicke, Phys. Rev. 93 (1954) 99.
[20] A.V. Andreev, V.I. Emel'yanov, Y.A. Il'inskii, Cooperative Effects in Optics: Superradiance and Phase Transitions, Institute of Physics Publishing, Bristol and Philadelphia, 1993.
[21] V.B. Pavlov-Verevkin, Phys. Lett. A 129 (1988) 168.
[22] P.A. Apanasevich, B.D. Fainberg, B.A. Kiselev, Opt. Spectrosc. 34 (1973) 101 (Opt. Spektrosk. 34 (1973) 209).
[23] P.A. Apanasevich, B.D. Fainberg, Opt. Spectrosc. 36 (1974) 1 (Opt. Spektrosk. 36 (1974) 3).
[24] B.D. Fainberg, Sov. Phys. JETP 42 (1976) 982 (Zh. Eksp. Theor. Fiz. 69 (1975) 1935).
[25] E. Fradkin, Field Theories of Condensed Matter Systems, Addison-Wesley, New York, 1991.
[26] D.B. Chesnut, A. Suna, J. Chem. Phys. 39 (1) (1963) 146.
[27] F.C. Spano, Phys. Rev. Lett. 24 (24) (1991) 3424.
[28] G. Li, B.D. Fainberg, A. Nitzan, S. Kohler, P. Hanggi, Phys. Rev. B 81 (16) (2010) 165310 [arXiv: 0910.4972 (cond-mat.str-e cond-mat.mes-hall)].
[29] P.O.J. Scherer, Adv. Mater. 7 (5) (1995) 451.
[30] V.L. Bogdanov, V.P. Klochkov, Opt. Spectrosc. 44 (1978) 412.
[31] V.L. Bogdanov, V.P. Klochkov, Opt. Spectrosc. 45 (1978) 51.
[32] V.L. Bogdanov, V.P. Klochkov, Opt. Spectrosc. 52 (1982) 41.
[33] F.C. Spano, S. Mukamel, Phys. Rev. A 40 (10) (1989) 5783.
[34] V.I. Likhopersky, Math. Modell. 12 (8) (2000) 91 (in Russian).